Atmos. Meas. Tech. Discuss., doi:10.5194/amt-2016-136, 2016
Manuscript under review for journal Atmos. Meas. Tech.
Published: 28 April 2016

Atmospheric Measurement Techniques Discussions

Observing relationships between lightning and cloud profiles by means of a satellite-borne cloud radar

Martina Buiat[1], Federico Porcù[2], Stefano Dietrich[3]

[1]University of Ferrara, Dept. of Physics and Earth Sciences, Ferrara, Italy
[2]University of Bologna, Dept. of Physics and Astronomy, Bologna, Italy
[3]Institute of Atmospheric Sciences and Climate (ISAC), National Research Council of Italy (CNR), Rome, Italy

Correspondence to: Federico Porcù (federico.porcu@unibo.it)

Abstract. Cloud electrification and related lightning activity in thunderstorms have their origin in the charge separation and resulting distribution of charged iced particles within the cloud. So far, the ice distribution within convective clouds has been investigated mainly by means of ground based meteorological radars. In this paper we show how the products from Cloud Profiling Radar (CPR) on board CloudSat, a polar satellite of NASA's Earth System Science Pathfinder (ESSP), can be used to obtain information from space on the vertical distribution of ice particles, ice content and relate them to the lightning activity.

The analysis has been carried out focusing on five convective events occurred over Italy that have crossed by CloudSat overpasses during significant lightning activity. The CPR products considered here are the vertical profiles of cloud Ice Water Content (IWC) and ice particles Effective Radius (ER), to be compared with the number of strokes as measured by a ground lightning network (LINET). Results show a strong correlation between the numbers of strokes and the vertical distribution of ice particles as depicted by the 94 GHz CPR products: in particular, cloud top IWC peaks and relatively high profile-averaged RE seems to be favourable to produce strokes.

1 Introduction

Lightning is an effect of cloud electrification, but the detailed mechanisms that cause the charge separation are still debated. However, the importance of cloud microphysical structure, in particular the ice water content, in this process is generally accepted and is confirmed by experimental studies and numerical modelling. Considering the various mechanisms, the non-inductive ice-ice interaction is one of the most accredited for cloud electrification. This mechanism requires the presence of large ice hydrometeors (i.e. graupel or hail pellets) that collide with ice crystals in a suspension of supercooled water droplets (Reynolds et al., 1957; Takahashi, 1978; Toracinta, 1995; Berdeklis and List, 2001). Jayaratne et al. (1983) showed that the charge sign could be positive or negative as a function of the cloud temperature, whereas positive cloud-to-ground (+CG) generally occur when the wind regimes increase in the storm evolution (MacGorman and Burgess, 1994). The hail portion of

Atmos. Meas. Tech. Discuss., doi:10.5194/amt-2016-136, 2016
Manuscript under review for journal Atmos. Meas. Tech.
Published: 28 April 2016

Atmospheric Measurement Techniques Discussions

a storm (Liu et al., 2009) and the tornado sightings in tornadic storms (Carey and Rutledge, 1998) are a couple of examples where the intensification of the event is coupled with the shift from –CG to +CG (MacGorman and Burgess, 1994).

Actually, the dominant source of in-cloud charge is the result of colliding ice particles, as described for example in Adamo et al. (2007). The convective updraft increases the liquid water content, the number of supercooled water droplets, and the number and size of ice crystals available in the so called charging zone, namely the region in which the charge transfer takes place. After collisions between rimed particles and smaller ice particles, the larger particles take one charge while the smaller ice crystals take the opposite. Larger particles such as hail and graupel remain suspended in the updraft and fall out when their terminal velocity exceeds the updraft, while the lighter ice particles are lifted to the upper regions of the cloud establishing an electric field within the cloud. This generates the in-cloud electric field distribution that initiates lightning when the field exceeds values of 100–250 kV m^{-1} (Marshall, Rust et al., 1995; Marshall, McCarthy et al., 1995).

The above conceptual model is the foundation for numerical models like the 1-D Explicit Microphysics Thunderstorm Model (Solomon and Baker, 1996; Solomon, 1997; Solomon et al., 2005) used to study the relationships between lightning activity and cloud microphysical structure (Formenton, 2013).

Since the relationship between lightning and microphysics is widely accepted, radar has frequently been used to investigate thunderclouds. Rutledge and Petersen (1994) confirmed with their observations the bipolar model described by Orville et al. (1988): the majority of the negative CG flashes are located in the region of higher radar reflectivity while the positive ones are found in areas of weaker reflectivity, in coincidence with the stratiform rainfall region.

Much research (since Kinzer, 1974) has been devoted to the observation of radar reflectivity and lightning considering the horizontal structure of the thundercloud. More recently, authors have begun to investigate the vertical structure of radar reflectivity. Rutledge and Petersen (1994) found that the number of cloud-to-ground flashes is highly correlated with the vertical radar profile, showing the contribution of the mixed-phase region to the non-inductive charging mechanism. Zipser et al. (1994) analysed the vertical profiles of radar reflectivity (VPRR) and the known differences in lightning frequencies for three different regimes (oceanic, monsoon and continental), confirming the relationship between the Ice Water Content (IWC) and the effectiveness of charge separation. More recently, Katsanos et al. (2007) confirmed the correlation between reflectivity and lightning, finding a vertical profile with values greater than 53 dBZ in the low levels, of ≈45 dBZ at 5 km and 40 dBZ at 7 km associated with an 80% probability of lightning occurrence. Deierling and Petersen (2008) and Deierling et al. (2008) used a Doppler and dual-polarimetric radar as a source of information of ice distribution and updrafts in clouds, in conjunction with lightning data collected in northern Alabama and Colorado/Kansas during two field campaigns. They found significant relationships between the total lightning activity and precipitating and nonprecipitating ice mass and estimated fluxes, as well as with updraft volume in the charging zone (i.e., for temperatures colder than − 5 °C), and found that these relationships are relatively invariant between different climate conditions. Roberto et al. (2016) found a marked relationship between cloud graupel content by using C-band radar. Radar reflectivity gradient is also a good indicator for strong updrafts (Toracinta, 1995;

Atmos. Meas. Tech. Discuss., doi:10.5194/amt-2016-136, 2016
Manuscript under review for journal Atmos. Meas. Tech.
Published: 28 April 2016

Zipser and Lutz, 1994; Hondl and Eilts, 1994), which contribute to the creation of opposite charge regions. Some clues in the same direction came also from satellite measurements. Petersen et al. (2005) pointed out that a solid relationship can be found between lightning and ice microphysics. In their study, they used the cloud ice microphysics information available from the Precipitation Radar (PR) onboard the Tropical Rainfall Measuring Mission (TRMM) spacecraft (2A25 PR product) to find global relationships between ice water content and lightning activity as observed by the LIS instrument onboard TRMM. They found that on a global scale the relationship between columnar precipitation ice mass and lightning flash density is invariant between land, ocean and coastal regimes (in contrast to rainfall).

However, PR uses a frequency (13.8 GHz) not optimal for taking into account contribution to the IWC due to small ice crystals in the upper cloud portion. More complete information about IWC profile can instead be provided by the so called cloud radars, active sensors at higher frequency. Ground based cloud radars generally provide a limited amount of information about the ice in convective clouds due to the signal attenuation caused by the underlying liquid particles and rain layers. On the contrary, satellite based cloud radars like the 94 GHz Cloud Profiling Radar (CPR) on CloudSat and planned on EarthCARE, have demonstrated their full potential in profiling IWC and RE (Stephens et al., 2008; Austin et al., 2008).

In this work, we propose a novel approach to study the relationship between lightning and the vertical distribution of IWC and ER, characterizing the charged cloud regions. We report statistical results obtained studying five convective events occurred over Italy, while one of them is analysed in detail to better describe the relationship between cloud structure and lightning occurrence.

2 Instruments and data

2.1 CloudSat CPR

CloudSat is a NASA Earth Sciences Systems Pathfinder mission started in 2006, and flies in formation with other Earth Sciences missions, taking part in a constellation of sun-synchronous satellites called "A-train" (Stephens et al., 2008). The overlap between the field of view of the satellites brings to a multi-satellite observing system for studying different aspects of the atmosphere. In particular, the objective of CloudSat is to measure for the first time the vertical structure of the clouds in order to improve their characterization in global models. The CloudSat instrument is the 94-GHz nadir-pointing CPR, which measures the power backscattered by targets as a function of distance from the radar. The CPR provides 2D atmospheric slices with a vertical resolution of 240 m, a 1.7x1.4 km footprint, and a sensitivity around -28 dB. The 3 mm wavelength provides sensitivity to light precipitation and both solid and liquid cloud particles, usually not detected by ground based low frequency weather radars (Stephens et al., 2008).

For this study, we used two 2B-level CloudSat products: the cloud geometrical profile (2B-GEOPROF) and the radar only version of the cloud ice and liquid water content (2B-CWC-RVOD). The 2B-GEOPROF contains the measured reflectivity of

Atmos. Meas. Tech. Discuss., doi:10.5194/amt-2016-136, 2016
Manuscript under review for journal Atmos. Meas. Tech.
Published: 28 April 2016

Atmospheric Measurement Techniques Discussions

the vertical column, after a screening performed with the MODIS cloud mask to filter out non cloudy profiles and a correction for gaseous absorption. The 2B-CWC-RVOD provides vertical profiles of IWC, LWC and cloud particle effective radius: the retrieval algorithms work on profiles already classified as cloudy and assumes lognormal cloud particles size distribution, using also the vertical temperature profile as estimated by ECMWF analysis (Stephens et al., 2008).

2.2 Lightning Location System data

Lightning strokes acquired by LINET (Betz et al., 2007; Betz et al., 2009) have been used in the study. LINET is a lightning detection network developed at the University of Munich in 2006 consisting of about 130 sensors ensuring a 200-250 km baseline in 17 European countries (Betz and Meneux, 2014). Most of VLF/LF lightning networks reports exclusively or dominantly CG strokes, while VHF methods allow the detection of in-cloud or cloud-to-cloud discharges (IC) (Nag et al., 2015). The two different signals relate to two distinct moments of a lightning: VHF emissions are associated with discharges fast in time and short in length, such as initial breakdown and stepped leader, while long channels, typical in CG but also present in IC, emit VLF/LF signals.

LINET works in VLF/LF band, but a lightning detection algorithm to discriminate IC from CG is applied as well. Even if CG and IC signals tend to dominate respectively at high and low currents (Betz et al., 2009), a discrimination based on amplitude considerations is not reliable due to the overlap between them (Nag and Rakov, 2008; Orville et al., 2002). For this reason a 3D-method, called Time of Arrival (TOA) has been developed. This method is based on the different origins of VLF emission between IC and CG: the corresponding differences in travel times are calculated by the TOA locating algorithm and give the height of the lightning emission. This method requires a maximum sensor baseline of 250 km and location accuracy sufficient to appreciate the difference of the two travel distances. The location accuracy has been verified by strikes into towers of known position (Betz et al., 2008) and reaches an average accuracy around 150 m. The comparison with other lightning networks has revealed a good time-coincidence (Loboda et al., 2009) and a higher capacity to discriminate IC from CG (Lagouvardos et al., 2009). The good sensitivity of the antenna, which detects signals smaller than 5 kA, attributes a total lightning quality to the network. The magnetic flux of the lightning signal is detected by means of two orthogonal loops directly as a function of time in a frequency range between 1 and 200 kHz, while signal timing is achieved by a GPS clock with accuracy better than 100 ns (Betz et al., 2009). This characteristic is useful for a variety of research purposes, such as cell tracking (Betz et al., 2008), recognition of severe weather conditions, the study of lightning induced chemical processes (Tuck, 1976), and guarantees an input for the improvement of models which describe convective processes. The algorithm analyses a window of 512 μs, i.e. no more than one event can be detected within this time period. Signals of technical origin are discriminated through a fast Fourier analysis (Betz et al., 2007).

Atmos. Meas. Tech. Discuss., doi:10.5194/amt-2016-136, 2016
Manuscript under review for journal Atmos. Meas. Tech.
Published: 28 April 2016

Atmospheric Measurement Techniques Discussions

3 Analysis of the relationship between cloud structure and lightning

To discuss the capability of CPR profiles to describe the cloud vertical structure in relationship with the number of lightning produced by the cloud, we selected five significant case studies occurred over Italy and well intercepted by the CloudSat overpasses. We first performed a statistical analysis on the whole dataset to evidence the role of ice structure of the cloud, and then focused on a case study optimally observed by CPR and characterized by a long term record of lightning.

3.1 Relationship between cloud vertical structure and number of strokes.

Five events with lightning observed by CPR over Italy have been selected to look for a direct dependence of the rate of strokes on the vertical cloud profile characteristics, as estimated by CPR reflectivity. For each cloud profile, a neighbourhood of 1.5 km radius is searched for strokes in the LINET database, within an interval of ±5 minutes around the time of the satellite overpass. In the five cases, we counted a total of 196 strokes, assigned to 56 profiles, out of a total of 1031 cloud profiles collected by CPR.

First, we analysed the IWC vertical distribution more favourable to produce strokes. Figure 1a presents the number of profiles with at least one stroke divided by the number of profiles for each interval of mean IWC profile, indicating that 0.5 g m^{-3} is a significant threshold to increase the occurrence of strokes from values below 20% to above 40%, but strokes may also occur for very low mean IWC. These values can be regarded as the frequency that one profile with a given mean IWC produces at least one stroke. In Figure 1b is shown the number of profiles with at least one stroke divided by the number of profiles for each interval of maximum value of the IWC measured along the profile: if the IWC maximum is below 1 g m^{-3} the relative stroke occurrence is below 20%, it increases up to 100% when the maximum IWC reaches 1.5 g m^{-3}. In Figure 1c is reported the number of profiles with at least one stroke divided by the total number of profiles as a function of the height of the IWC maximum for the profile. When the maximum IWC is located at higher levels a greater stroke occurrence is found: all the 3 profiles with the IWC maximum above 11.5 km have strokes. The distribution shows that the strokes occurrence is favoured in profiles with IWC peak above 5 km, and generally, the main IWC peak is located in the middle cloud layers, around 7 km (for the 30.4% of the total profiles with strokes) or at the cloud top, around 11 km (for the remaining 69.6%), while profiles with IWC peak around 9 km are less prone to produce strokes.

The second CloudSat product we analysed in order to characterize the cloud profiles is the ER of the ice particles, defined as the ratio between third and second order moment of the particle size distribution, i.e. the area-weighted mean of the particle radius (Hansen and Travis, 1974). It is worth noting that when non-spherical ice particles are concerned, the particle radius means the radius of the equivalent mass ice sphere. In Figure 2a is shown the number of profiles with at least one stroke divided by the number of profiles for each interval of mean ER. A relatively high mean ER (larger than 0.95 mm) indicates higher probability to have strokes, while the same fraction distributed over the maximum ER in the profiles, reported in figure 2b, presents a peak between 1.3 and 1.35 mm, indicating that few layers with large ER are not essential to have strokes. CPR is

Atmos. Meas. Tech. Discuss., doi:10.5194/amt-2016-136, 2016
Manuscript under review for journal Atmos. Meas. Tech.
Published: 28 April 2016

Atmospheric Measurement Techniques Discussions

not conceived to classify hydrometeor types, but large mean values of ER are likely related to the presence of graupel in a significant part of the cloud profile.

Finally, we compared our results to similar studies carried on by using ground-based, C-band weather radar applied to severe events in Italy (Roberto et al., 2016), global TRMM-based climatology (Petersen et al., 2005), and numerical simulations (Formenton et al., 2013). In Figure 3 are reported, for the five events considered here, the values of the event-averaged Ice Water Path (IWP) and the flashes spatial density at the time of CPR observation ± 5 min. On the same plot are reported the minimum threshold linear function proposed by Formenton et al. (2013) and the linear relation found by Petersen et al. (2005) over land (both converted to match the units used for this plot). These two lines express the relationship between IWP and flash density: the first one, based on numerical modelling takes into account only the contribution of graupel to IWP, while the second is based on global observation of LIS and PR on TRMM, and considers the total IWP. The three more lines in Figure 3 represents the regression lines of three events analysed by Roberto et al. (2016) with a ground based, C-band radar, where only the graupel contribution is used to compute the cloud-averaged IWP. In order to compare all these results, we have grouped strokes into flashes using the Yair et al. (2014) approach: strokes recorded in 1 km^2 within 0.2 s were grouped into one flash.

Three of our experimental points lay above all the lines, while two events are described by the Petersen et al. (2005) line. The peculiarity of our study is that CPR measures also the contribution of smaller ice crystals in the upper part of the cloud to the IWP, which is not considered by Ku- (TRMM-PR) and C-band (ground weather radar) instruments, due to lower sensitivity. Our result show that, in general, there is a proportional relationship between IWP and flash density, with some difference with previous studies. There is a substantial agreement with the Petersen et al. (2005) line, this because both studies makes use of satellite borne radars and do not apply hydrometeor classification, while the other lines refer more directly to graupel content. This is an indication that the 2D vertical cloud section provided by CPR contains sufficient information to be compared with the TRMM-PR 3D scanning. For the two events laying on the Petersen et al. (2005), the IWP is mainly due to large ice particles (snowflakes, graupel and hailstones), while for the other three a not negligible part of the contribution to the IWP comes from small ice particles. To better illustrate these findings, we carried out a deeper study on one of these later cases and the results are presented in the next section.

3.2 Case study occurred on 12-13 August 2010

To have a deeper look into the cloud profiles structure favourable to lightning development, we selected one case study of a mesoscale organized, long lasting convective system that occurred in Northern Italy on the night between August 12th and 13th 2010. The convective episode started in late afternoon (LT) of August 12th above the western Po Valley and moved eastward in the following hours, reaching the maximum development around 23:30 UTC the same day. This event produced a long time record in terms of number of strokes in northern Italy.

Atmos. Meas. Tech. Discuss., doi:10.5194/amt-2016-136, 2016
Manuscript under review for journal Atmos. Meas. Tech.
Published: 28 April 2016

Atmospheric Measurement Techniques Discussions

In Figure 4 the METOSAT-9 10.8 μm image at 01:27 UTC is reported in colour shades, with superimposed (in black) the pixels where lightning activity was registered by LINET network within 10 min interval centred on the image acquisition time, as described in the previous Section. The dashed black line indicates the track of the CloudSat orbit that overpasses the area of interest at 01:29 UTC. The segment from A to B is the portion of the orbit considered in this study. The case study and the orbit was selected because very close to the electrically active portion of the cloud and also capable to sample the anvil region, where no strokes were detected by LINET during the specific 10 minutes interval.

In Figure 5, the CPR reflectivity is plotted in colour shades along the path shown in Figure 4, while the bars below indicate the number of strokes registered by the LINET in the corresponding profiles. The structure of the cloud shows a well-developed anvil stretching to the north and the convective activity on the south. A thick, highly reflecting cloud ice layer is present: the top of the cloud reaches 12 km a.s.l., while high ice water content (above 0.8 g m^{-3}, not shown) columns reach 5 km a.s.l. It has to be remarked that CPR signal could be strongly attenuated by large hydrometeors and thus the lower cloud layers and rain structures are expected to be not properly described by CPR profiles.

Lightning activity occurs only on the convective part of the cloud, while no strokes are detected on the anvil and also in the growing convective cell at around profile n. 30 along the track. However, there is a relatively large region (between profile n. 98 and profile n. 110) where no strokes are recorded despite the CPR reflectivity shows a thick cloud layer: this suggests that not only the high ice content is a key factor in developing strokes, but also the vertical distribution of IWC has an impact. Out of the total number of strokes detected (82) only three are positive, and are detected in the area of weakest reflectivity, which corresponds to the stratiform rainfall region, confirming the model described by Orville (Orville et al., 1988).

To understand better the role of IWC vertical distribution, a more detailed analysis is made by selecting profiles with and without lightning and in the convective part of the cloud. In Figure 6, vertical profiles of CPR products IWC and ER are presented in case of lightning detected (top panel) and no lightning detected (bottom panel) in proximity of the profiles. Figure 6a shows the profile n. 96 from the start of the cross section reported in Figure 5, where the LINET registered 13 strokes, while 12 strokes are reported for the profile n. 118, shown in Figure 6b. For Figures 6c (profile n. 106) and 3d (profile n. 124), still in the active part of the cloud, no strokes are reported. The cloud structures in these four cases present some similarities: thick ice layer between 5 and 11 km above the ground with peak concentration larger than 1 g m^{-3} at about 10 km above the ground. The vertical distribution of ice content seems to be more related to the cloud capability to produce strokes: for no lightning cases the ice content decreases monotonically below the concentration peak until it vanishes reaching the melting layer (estimated around 3.7 km a.s.l.). In case of strokes, the IWC structure presents a secondary concentration peak at about 7 km a.s.l., at the same height where a peak of ER is present, indicating the possible presence of graupel.

Atmos. Meas. Tech. Discuss., doi:10.5194/amt-2016-136, 2016
Manuscript under review for journal Atmos. Meas. Tech.
Published: 28 April 2016

The presence of lightning is favoured by a dense ice layer at the cloud top, where relatively smaller ice particles are present, coupled with a second layer of high IWC, characterized by larger hydrometeors. This structure is coherent with the graupel-crystal charging mechanism.

4. Conclusions

Despite the difficulties in picking out CloudSat overpasses intersecting active convective cells in Italy, the combined use of lightning data together with the values of IWC provided by the CPR has highlighted the importance of the ice phase in the mechanisms that lead to the separation of charges in the cloud.

Statistical analysis based on five events show that a high mean and maximum IWC content is required to have strokes, possibly with peaks at around 7 km (Katsanos et al., 2007) or 10-11 km, while large values of profile averaged RE also favour strokes production. Comparisons with previous studies indicate that the contribution of small ice particles in the highest cloud layers should be taken into account to fully describe the relationship between vertical cloud structures and lightning.

From in-depth analysis of the selected case study, we have identified two distinct regions in the cloud structure favourable to lightning production. The upmost region is found at an altitude of about 10 km a.s.l., and is characterized by high values of IWC (above 1 g m^{-3}), with ER below 1 mm. The second region is characterized by a secondary IWC peak around 7 km a.s.l.: in this layer the cloud particles effective radius reaches the maximum, indicating the presence of larger ice hydrometeors (e.g. graupel). The profiles with no-lightning do not show this secondary peak in IWC, even if a peak in ER is found around 7 km a.s.l. These structures are coincident with the charge regions, which characterize the dipole, confirming the effectiveness of the mechanism of electrification non-inductive type of particle-particle: the ice crystals, positively charged, are pushed upward by the updraft, while the larger hydrometeors, negatively charged, are maintained in the lower part of the cloud.

Acknowledgements

CloudSat Standard Data Products are distributed by the CloudSat Data Processing Center, located at the Cooperative Institute for Research in the Atmosphere at Colorado State University in Fort Collins, within the NASA CloudSat Project. LINET data have been provided by Nowcast GmhB (https://www.nowcast.de/) within a scientific agreement between Prof. H.-D. Betz and the Satellite Meteorological Group of CNR-ISAC in Rome.

References

Adamo, C., Solomon, R., Medaglia, C. M., Dietrich, S. and Mugnai, A.: Cloud Microphysical Properties from the Remote Sensing of Lightning within the Mediterranean, In: Levizzani, V., Bauer, P. and Turk, J.: Measuring precipitation from space: EURAINSAT and the future, 127-134, Springer, 2007.

Austin, R.T., Heymsfield, A.J. and Stephens, G.L.: Retrieval of ice cloud microphysical parameters using the Cloudsat mm-wave radar and temperature, J. of Geophysical Res.: Atmospheres, 114, doi: 10.1029/2008JD010049, 2008.

Berdeklis, P. and List, R.:The ice crystal-graupel collision charging mechanism of thunderstorm electrification, J. of Atmos. Sci., 58, 2751-2770, doi: 10.1175/15202, 2001.

Betz, H.D. and Meneux, B.: LINET systems - 10 years experience, in International Conference on Lightning Protection (ICLP), 1553-1557, doi: 10.1109/ICLP.2014.6973377, 2014.

Betz, H.-D., Marshall, T. C., Stolzenburg, M., Schmidt, K., Oettinger, W. P., Defer, E., Konarski, J., Laroche P. and Dombai, F.: Detection of in-cloud lightning with VLF/LF and VHF networks for studies of the initial discharge phase, Geo. Res. Letters, 35, doi: 10.1029/2008GL035820, 2008.

Betz, H.-D., Schmidt, K., Fuchs, B., Oettinger, W. P. and Holler, H.: Cloud lightning: Detection and utilization for total-lightning measured in the VLF/LF regime, J. of Lightning Res., 2, 1–17, 2007.

Betz, H.-D., Schmidt, K., Laroche, P., Blanchet, P., Oettinger, Defer, E., Dziewit, Z.and Konarski, J.: LINET – An international lightning detection network in Europe," *Atmospheric Research*, vol. 91, pp. 564–573, 2009, doi: 10.1016/j.atmosres.2008.06.012, 2008.

Carey, L. D. S. and Rutledge, A.: Electrical and multiparameter radar observations of a severe hailstorm, J. of Geo. Res., 103(12), 13979–14000, doi: 10.1029/97JD02626, 1998.

Deierling, W. and Petersen, W. A.: Total lightning activity as an indicator of updraft characteristics, J. of Geo. Res., 113, doi: 10.1029/2007JD009598, 2008.

Deierling, W., Petersen, W. A., Latham, J., Ellis, S. and Christian, H.: The relationship between lightning activity and ice fluxes in thunderstorms, J. of Geo. Res., 113, doi: 10.1029/2007JD009700, 2007.

Formenton, M., Panegrossi, G., Casella, D., Dietrich, S., Mugnai, A., Sanò, P., Di Paola, FBetz,, H.-D., Price, C. and Yair, Y.: Using a cloud electrification model to study relationships between lightning activity and cloud microphysical structure, Natural hazards and earth system sciences, 13, 1085-1104, doi:10.5194/nhess-13-1085, 2013.

Hansen, J.E and Travis, L.D.: Light scattering in planetary atmospheres, Space Science Reviews, 16 (4), 527–610, doi: 10.1007/BF00168069, 1974.

265 Hondl, K. D., and Eilts, M. D.: Doppler radar signatures of developing thunderstorms and their potential to indicate the onset of cloud-to-ground lightning, Mon. Weather Rev., 122, 1818-1836, doi: 10.1175/1520-0493, 1994.

Jayaratne, E. R., Saunders, C. P. R. and Hallett, J.: Laboratory studies of the charging of soft hail during ice crystal interactions, Q. J. of the Royal Met. Soc., 109, 609–630, doi: 10.1002/qj.49710946111, 1983.

Katsanos, D. K., Lagouvardos, K., Kotroni, V. and Argiriou, A. A.:The relationship of lightning activity with microwave
270 brightness temperature and spaceborne radar reflectivity profiles in the central and eastern Mediterranean, J. of App. Met. and Clim., 46, 1901-1912, doi: 10.1175/2007JAMC1454.1, 2007.

Kinzer, G. D.: Cloud-to-ground lightning versus radar reflectivity in Oklahoma thunderstorms, J. of the Atmos. Sci., 31 (3), 787-799, doi: 10.1175/1520, 1974.

Lagouvardos, K., Kotroni,V.,. Betz, H.-D. and Schmidt, K.: A comparison of lightning data provided by ZEUS and LINET
275 networks over Western Europe, Nat. Hazards Earth Syst. Sci., 9, 1713-1717, 2009.

Liu, D., Feng, G. and Wu, S.: The characteristics of cloud-to-ground lightning activity in hailstorms over northern China, Atmos. Res., 91, 459-465, doi: 10.1016/j.atmosres.2008.06.016, 2009.

Loboda, M., Betz, H.-D., Baransky, P., Wiszniowski, J. and Dziewit, Z.: New Lightning Detection Networks in Poland – LINET and LLDN, The open Atmos. Sci. J., 3, 29-38, doi: 1874-2823/09, 2009.

280 Mac Gorman, D.R. and Burgess, D.W.: Positive cloud-to-ground lightning in tornadic storms and hailstorms, Mon.Wea.Rev, 122, 1671-97, doi: 10.1175/1520-0493, 1994.
MacGorman, D. R. and Burgess, D. W.: Positive cloud-to-ground lightning in tornadic storms and hailstorms, Mon. Weather Rev., 122, 1671–1697, doi: 10.1175/1520, 1994.

Marshall, T. C., McCarthy, M. and Rust, W. D.: Electric field magnitudes and lightning initiation in thunderstorms, J. of Geo.
285 Res., 100, 7097–7103, doi: 10.1029/95JD00020, 1995.

Marshall, T. C., Rust, W. D. and Stolzenburg, M.: Electric structure and updraft speeds in thunderstorms over the Southern Great Plains, J. of Geo. Res., 100, 1001–1015, doi: 10.1029/94JD02607, 1995.

Nag, A. and Rakov, V. A.: Pulse trains that are characteristic of preliminary breakdown in cloud-to-ground lightning but are not followed by return stroke pulses, J. of Geo. Res., 113, doi: 10.1029/2007JD008489, 2007.

290 Nag, A., Murphy, M. J., Schulz, W. and Cummins, K. L.: Lightning locating systems: Insights on characteristics and validation techniques, Earth and Space Science, 2, doi: 10.1002/2014EA000051, 2015.

Orville, R. E., Burrows, W. R., Holle, R. L. and Cummins, K. L.:The north american lightning detection network (NLDN) – First results: 1998-2000, Mont. Weather Rev., 130, 2098-2109, doi: 10.1175/1520, 2002.

Orville, R. E., Henderson, R. W. and Bosart, L. F.: Bipole patterns revealed by lightning locations in mesoscale storm systems, Geo. Res. Lett., 15 (2), 129-132, doi: 10.1029/GL015i002p00129, 1988.

Petersen, W. A., Christian, H. J. and Rutledge, S. A.: TRMM observations of the global relationship between ice water content and lightning, Geo. Res. Letters, 32, doi: 10.1029/2005GL023236, 2005.

Reynolds, S. E., Brook, M. and Gourley, M. F.: Thunderstorm charge separation, J. of Meteorology, 14, 426-436, doi: 10.1175/1520, 1957.

Roberto, N., Adirosi, E., Baldini, L., Casella, D., Dietrich, S., Gatlin, P., Panegrossi, G., Petracca, M., Sanò, P. and Tokay, A.: Multi-sensor analysis of convective activity in central Italy during the HyMeX SOP 1.1, Atmos. Meas. Tech., 9, 535–552, doi:10.5194/amt-9-535-2016, 2016.

Rutledge, S. A. and Petersen, W. A.: Vertical radar reflectivity structure and cloud-to-ground lightning in the stratiform region of MCS's: Further evidence for in-situ charging in the stratiform region, Mon. Weather Rev., 122, 1760–1776, doi: 10.1175/1520, 1994.

Solomon, R. and Baker, M.: A one-dimensional lightning parameterization, J. of Geo. Res., 101, 14983–14990, doi: 10.1029/96JD00941, 1996.

Solomon, R., Medaglia, C. M., Adamo, C., Dietrich, S., Mugnai, A. and Biader, U.: An Explicit Microphysics Thunderstorm Model, Int. J. of Modelling & Simulation, 25, 112-118, ISSN: 0228-6203, 2005.

Solomon, R.: A modelling study of thunderstorm electrification and lightning flash rate, PhD Dissertation, Atmospheric Science Program, University of Washington, Seattle, Washington, USA, 1997.

Stephens G.L., Vane, D. G., Boain, R., J., Mace, G. G., Sassen, K., Wang, Z., Illingworth, A. J., O'Connor, E. J., Rosasaow, W., B., Durden, S. L., Miller, S., D., Austin, R., T., Benedetti, A. and Mitrescu, C.: The Cloudsat mission and the A-Train. A new dimension of space-based observation of clouds and precipitation, A. Met. Soc., 1771-1790, doi: 10.1175/BAMS-83-12-1771, 2002.

Stephens, G. L.,Vane, D. G., Tanelli, S., Im, E., Durden, S., Rokey, M., Reinke, D., Partain, P., Mace, G. G., Austin, R., L'Ecuyer, T., Haynes, J., Lebsock M., Suzuki, K., Waliser, D., Wu, D., Kay, J., Gettelman, A., Wang, Z., and Marchand, R.: CloudSat mission: Performance and early science after the first year of operation, , J. of Geo. Res., 113, doi: 10.1029/2008JD009982, 2008.

320 Takahashi, T.: Riming electrification as a charge generation mechanism in thunderstorms, J. of Atmos. Sci., 35, 1536-1548, doi: 10.1175/1520-0469, 1978.

Toracinta, E. R.: Radar, satellite, and lightning characteristics of select mesoscale convective systems in Texas, Master's thesis, A&M University, 1995.

Tuck, A. F.: Production of nitrogen oxides by lightning discharges, Q. J. of the Royal Met. Soc., 102, 749–755, doi: 325 10.1002/qj.49710243404, 1976.

Yair, Y., Shalev, S., Erlich, Z., Agrachov, A., Katz, E., Sarooni, H., Price, C., and Ziv, B.: Lightning flash multiplicity in eastern Mediterranean thunderstorms, Nat. Hazards Earth Syst. Sci., 14, 165-173, doi: 10.5194/nhess-14-165-2014.

Zipser, E. and Lutz, K. R.: The vertical profile of radar reflectivity of convective cells: a strong indicator of storm intensity and lightning probability?, Mon. Weather Rev., 122, 1751-1759, doi: 10.1175/1520, 1994.

330

335

340

Atmos. Meas. Tech. Discuss., doi:10.5194/amt-2016-136, 2016
Manuscript under review for journal Atmos. Meas. Tech.
Published: 28 April 2016

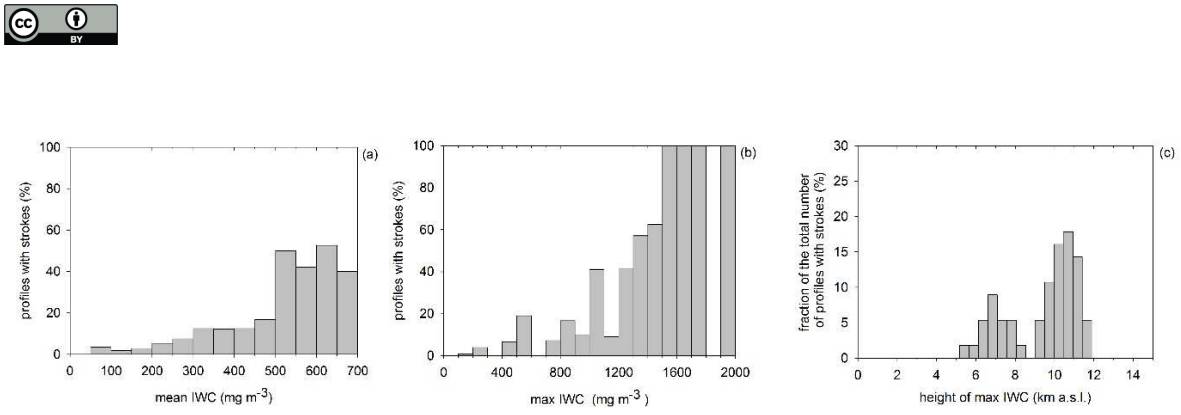

Figure 1: (a) Fraction of profiles with at least one stroke as a function of the mean IWC of the profile; (b) same quantity distributed according to the maximum value of the IWC along the profile; (c) same quantity distributed according the height of the maximum IWC.

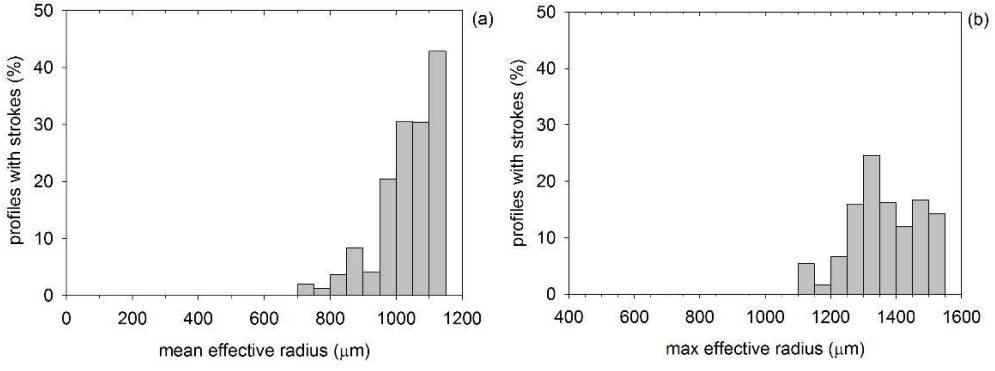

Figure 2: (a) fraction of profiles with at least one stroke as a function of the mean ER of the profile; (b) same fraction as a function of the maximum effective radius in the profile.

Atmos. Meas. Tech. Discuss., doi:10.5194/amt-2016-136, 2016
Manuscript under review for journal Atmos. Meas. Tech.
Published: 28 April 2016

Atmospheric Measurement Techniques Discussions

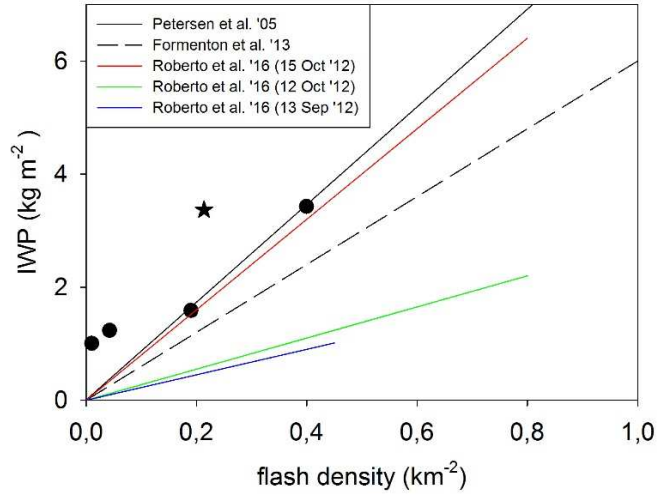

Figure 3: IWP averaged for the five events considered as function of flash density (black symbols: the star indicates the case study analyzed in the next Section). The black solid line is the linear relation found by Petersen et al. (2005) over land, the black dashed line is the threshold found by Formenton et al. (2013) and the red, green and blue lines are the results found by Roberto et al. (2016) with a ground based, C-band radar for three events.

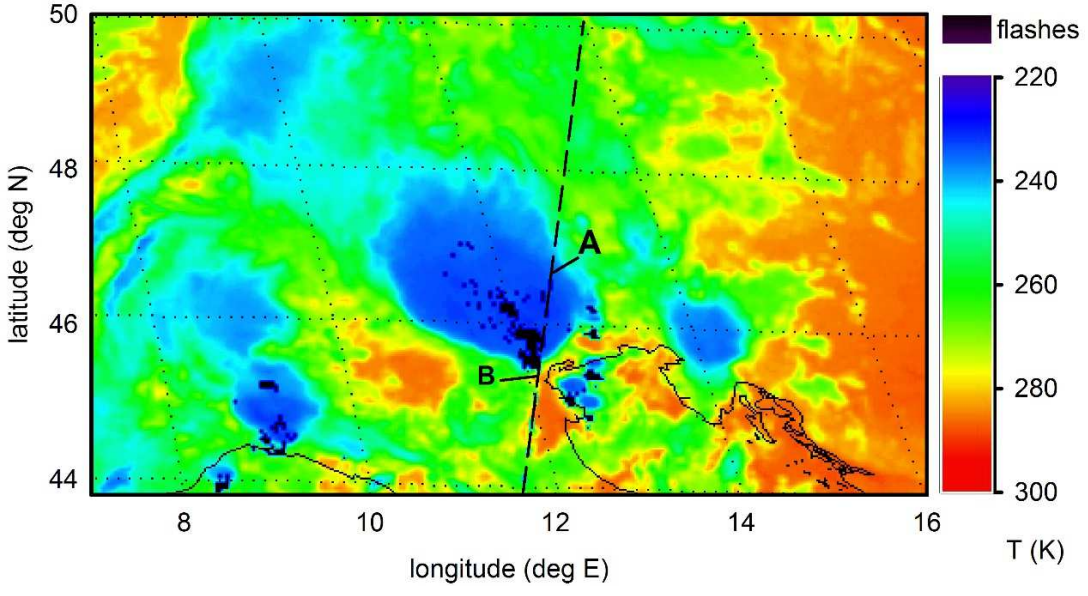

Figure 4. The 10.8 μm METEOSAT SEVIRI image at 01:27 UTC on August 13 2010 centred on the analysed cloud system. Dashed line indicates the track of CloudSat orbit, A and B indicate the beginning and the end, respectively, of the vertical cross section shown in Figure 5.

Atmos. Meas. Tech. Discuss., doi:10.5194/amt-2016-136, 2016
Manuscript under review for journal Atmos. Meas. Tech.
Published: 28 April 2016

Atmospheric Measurement Techniques Discussions

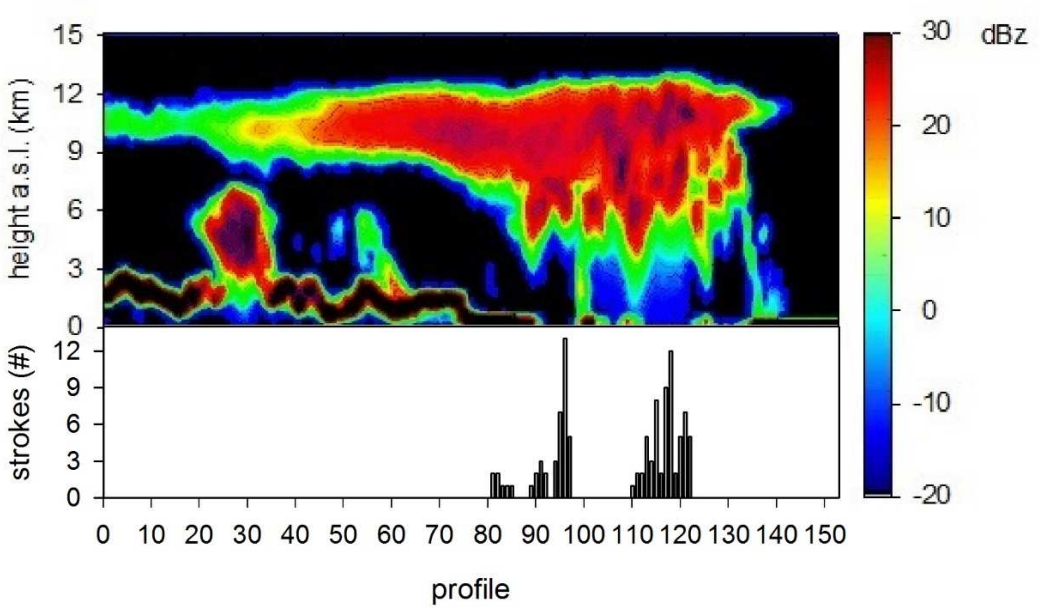

Figure 5: Vertical cross section of the CPR reflectivity along the path shown in Figure 4. In the bottom panel, the number of strokes recorded by LINET for each CPR profile are reported.

Atmos. Meas. Tech. Discuss., doi:10.5194/amt-2016-136, 2016
Manuscript under review for journal Atmos. Meas. Tech.
Published: 28 April 2016

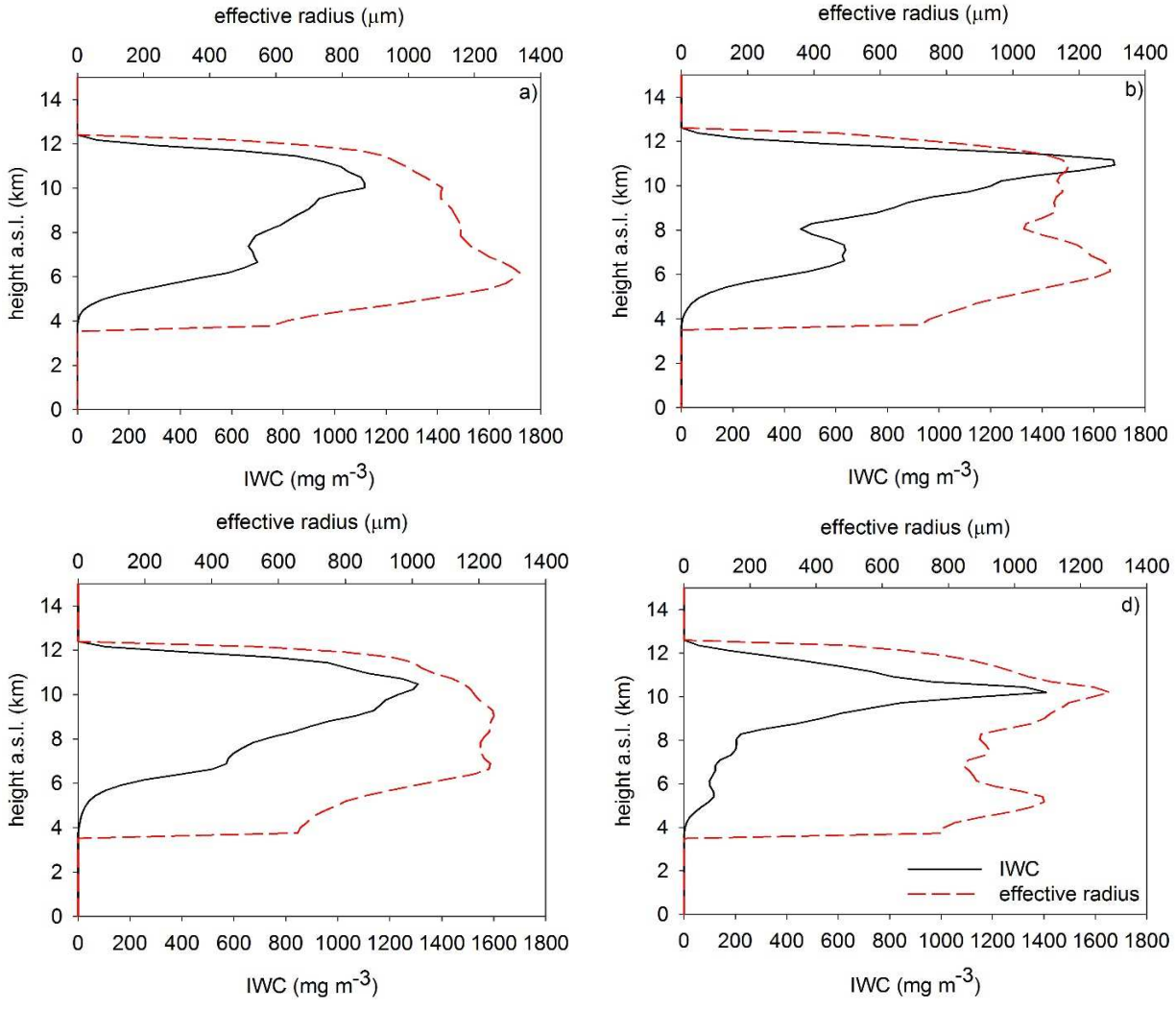

380

Figure 6. Vertical profiles of IWC (black line, bottom axis) and ER (red line, top axis) for four CPR profiles, namely: (a) n. 96 (13 strokes), (b) n. 118 (12 strokes), (c) n. 106, and (d) n. 124 (zero strokes).